Experimental and finite elements analysis of the vibration behaviour of a bio-based composite sandwich beam

Arthur Monti, Abderrahim El Mahi, Zouhaier Jendli, Laurent Guillaumat

Experimental and finite elements analysis of the vibration behaviour of a bio-based composite sandwich beam

Arthur Monti [a, *], Abderrahim El Mahi [a], Zouhaier Jendli [b], Laurent Guillaumat [c]

[a] LAUM - Laboratoire d'Acoustique de l'Université du Maine, Avenue Olivier Messiaen, 72085 Le mans Cedex 9, France
[b] ESTACA'Lab – Pôle Mécanique des Matériaux Composites et Environment, Parc Universitaire Laval-Changé, Rue Georges Charpak, BP-76121, 53061 Laval Cedex 9, France
[c] LAMPA - Laboratoire Angevin de Mécanique Procédés et innovAtion, Arts et Métiers ParisTech Campus Angers 2, Boulevard du Ronceray, 49035 Angers Cedex 01, France

Keywords:
Mechanical testing
Vibration
Finite element analysis (FEA)

A B S T R A C T

This paper presents the results of experimental and numerical analyses of the flexural vibration behaviour of bio-based sandwich structures and their composite faces, and particularly their damping properties. The material studied is made up of two skins made of a thermoplastic matrix reinforced by flax fibres and a balsa wood core. The faces and the whole sandwich structures were produced by liquid resin infusion. First, experimental tests were performed on the skins. Free vibration tests were carried out on unidirectional and cross-ply laminates in a clamped free configuration to investigate the influence of the fibre orientation and stacking sequence on the dynamic stiffness and loss factors. Then, the damping behaviour of the balsa core was studied through several free vibration tests. In addition, the damping properties of sandwich beams with different thicknesses were measured and discussed. Finally, a finite elements model was used to calculate the resonance frequencies and modal loss factors of different sandwich beams. Close correlation between the numerical and experimental results was observed. Finally, a modal strain energy method was used to evaluate the contribution of the skins and of the core to the damping properties of the different sandwich beams.

1. Introduction

In the past decades, bio-based composites have proven to be very interesting materials to face some current engineering challenges, such as the achievement of lightweight structures in automotive, aeronautics, marine and other transportation industries. Among them, natural fibre reinforced polymers (NFRP) exhibit very interesting specific properties (stiffness or strength to mass ratios) [1–4]. For this reason, a significant amount of research activities has been conducted on composites reinforced with agro based fibres. In Europe and particularly in France, flax fibre reinforced polymers (FFRP) are among the most commonly studied eco-composites [5,6]. As a matter of fact, they exhibit specific properties comparable with those of traditional glass fibre reinforced polymers (GFRP) [7]. Moreover, the use of such bio-based components can reduce the impact of the final product on the environment. In the same way, thermoplastic matrices are also often used in order to achieve recyclable composite parts [8–11]. In addition, some 100% bio-based thermoplastic materials associated with plant fibres can lead to biodegradable composites [12], opening new perspectives for the end-of-life management of these materials.

In parallel with the development of eco-friendly composites, sandwich structures are widely used in weight critical applications [13,14]. They are made up of two stiff and strong skins associated with a light core whose thickness increases the quadratic moment of the sandwich structure. This improves the flexural stiffness and strength of the beam with only minimal impact on its mass. Thus, the use of bio-based materials should allow the production of sandwich structures with high specific properties as well as reducing their environmental impact. Nowadays, balsa wood is among the most commonly found eco-product used as a core material. Several authors have highlighted interesting properties for balsa cored sandwiches, sometimes even coupled with bio-based composite skins. Le Duigou et al. [15,16] have studied a structure made of PLLA/Flax skins and balsa core. Beside interesting

* Corresponding author.
E-mail address: arthur.monti.etu@univ-lemans.fr (A. Monti).

http://dx.doi.org/10.1016/j.compositesb.2016.11.045

specific properties, the authors also emphasize a lower environmental impact for this eco-material than for traditional glass/polyester sandwiches. Moreover, some authors have proposed modifications of classic balsa panels to improve the core shear properties [17,18]. In addition, balsa wood has proven to be good at absorbing impact energy [19]. Kandare et al. also proved that a sandwich structure made of flax/epoxy skins and a balsa core is fire retardant [20]. Notwithstanding these numerous analyses, it is surprising how few references exist concerning the vibration properties of bio-based sandwich structures with balsa cores and NFRP skins. However, several authors have already shown that the use of plant reinforcements improves the damping properties of composites [21–23]. Thus, natural fibres are sometimes coupled with carbon or glass fibres to achieve hybrid damping materials [24]. Sargianis et al. [25] studied several configurations of sandwich beams with bio-based cores and skins. These structures exhibited superior acoustic properties with minimal sacrifices in stiffness and strength to mass ratios. Regarding these conclusions, bio-based sandwich structures could also bring new perspectives in terms of damping solutions. Due to their inherent ability to absorb energy, their use could enrich the common state of the art methods to damp vibrations, which most commonly consist in adding local passive or active dampers to the structures, increasing their mass and cost.

In this context, this work presents the results of an experimental and numerical analysis of the vibration behaviour of a bio-based sandwich structure. The material is made of a balsa core and thermoplastic skins reinforced by flax fibres. The matrix used is an innovative thermoplastic resin developed for the manufacturing of composite parts by liquid resin processes such as resin transfer moulding. The aim of this work is to emphasize the good vibration damping properties of this kind of sandwich structures. The roles of the skins and core in the energy dissipation mechanisms are analysed through experimental investigations and numerical simulations.

2. Materials and experimental setup

2.1. Materials and manufacturing

The reinforcement used here is a tape of unidirectional continuous flax fibres (FlaxTape) provided by LINEO [26]. The long fibres are held together without any twisting or transverse fibres by a process based on the reactivation of external pectin cements on the surface of fibre bundles. They are associated with an innovative thermoplastic resin (Elium®) provided by ARKEMA, developed for the manufacturing of thermoplastic composite parts by liquid resin processes such as resin transfer moulding (RTM) or liquid resin infusion (LRI). This acrylic resin is activated by peroxide (2% CH50x). In addition, the core of the sandwich structure is made of balsa wood. The balsa panels used, provided by SICOMIN, are cut with a regular pattern to facilitate the resin infusion. Such panels can also be used for the manufacturing of curved structures. A density of 150 kg m^{-3} was used, with several thicknesses to achieve different sandwich beam configurations. To manufacture the laminates, four layers of flax tapes with a surface mass of 200 gr m^{-2} are initially dried in a ventilated oven at 110 °C for one hour [27]. Then, they are laid out on a clean waxed mould in the desired stacking sequence. An infusion mesh is added on the top of them to increase the permeability of the medium. In addition, a peel ply is used to facilitate separating the composite from the infusion materials. This stack of dry plies is then covered by an impermeable flexible film, fixed to the mould by an adhesive sealer. This vacuum bag contains a resin inlet and an outlet connected to the vacuum pump. Before infusion, maximum vacuum is maintained for one hour to allow the degassing of the fibres. Then, vacuum is set to 0.5 bars and the resin inlet is opened. Thus, the catalysed resin is distributed through the infusion mesh and impregnates the fibres. At the end of the infusion process, the resin inlet is closed. The final part is generally demoulded after 24 h. Previous mechanical studies [28] have given the mechanical properties presented in Table 1, obtained for a flax/elium® UD composite with a fibre volume fraction equal to 35%.

Sandwich panels are produced by the same method. To facilitate the resin circulation, an infusion mesh and a peel ply are added between the mould and the fibres which constitute the lower skin. Thus, the catalysed resin entering the inlet separates into two flows below and above the sandwich structure. The gaps between adjacent balsa strips also contribute to the circulation of the resin between the lower and upper faces.

For this study, several configurations of laminates were prepared. Unidirectional beams with nominal dimensions 300 mm × 20 mm ×1.6 mm were produced with 0 °, 45 ° and 90 ° oriented fibres in order to study the influence of fibre orientation on the damping properties of the material. They were labeled UD-0, UD-45 and UD-90 respectively. Their properties were compared to those of pure resin specimen with nominal dimensions 200 mm × 20 mm × 2.5 mm. Moreover, cross-ply laminates with $[0/90]_s$ and $[+45/-45]_s$ layups were prepared to emphasize the influence of the stacking sequence. In addition, tests were performed on balsa beams with the following dimensions: 300 mm × 40 mm × 15.9 mm to figure out its dynamic behaviour under longitudinal and shear vibrations. Finally sandwich beams with a nominal length of 340 mm and a nominal width of 40 mm made of flax/Elium® composites and balsa wood were produced with several core thicknesses (6.4 mm, 12.7 mm, 15.9 mm and 19.1 mm). For all of them, the skins were made of 4 flax plies (1.6 mm thick) with $[0/90]_s$ stacking.

2.2. Free vibration experimental setup

To study the vibration behaviour of the composite and sandwich beams, free vibration tests were carried out with the apparatus presented in Fig. 1. Beams were tested in a clamped-free configuration, according the standard ASTM E−756 [29]. The clamping length was set to 40 mm. To avoid damaging the core while clamping sandwiches, 40 mm of balsa was replaced by metallic inserts. The beams were excited by an impact hammer (PCB084A14) close to the clamped end. The displacement of the free end was measured by a laser vibrometer (OFV 303 Sensor Head). The excitation and response signals were processed by an acquisition card system and analysed with the NVGate software. Tests were performed at room temperature and humidity. For each beam, the vibration tests were repeated several times and the five best signals were averaged to produce the final data sets. Moreover, to take into account the potentially scattered properties of these natural materials, a minimum of 6 beams for each configuration of

Table 1
Mechanical properties of Flax/Elium UD beams.

E_1(GPa)	E_2(GPa)	E_{45}(GPa)	G_{12}(GPa)	σ_1(MPa)	σ_2(MPa)	σ_{45}(MPa)	σ_{12}(MPa)	ν_{12} (−)
23,3	3,2	3,65	1,5	230	8	12	14	0,35

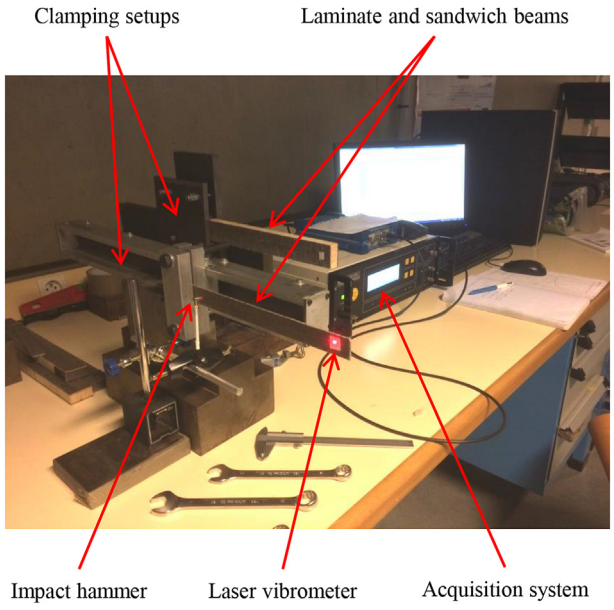

Fig. 1. Experimental setup for free vibration analysis of clamped-free composite and sandwich beams.

laminates were tested. Due to the amount of material and work required to prepare the sandwich structures, 3 beams at least were tested in all configurations. Then, the data was processed with MATLAB software to generate the beam frequency response function (FRF). An automatic routine was then applied to each FRF to detect resonance peaks. For all of them, Bode and Nyquist diagrams were plotted. A typical example, corresponding to a sandwich beam with $[0/90]_s$ skins and a 15.9 mm thick core is given in Fig. 2 a. In this case, five resonance modes can be distinguished. In the Nyquist plane which presents the imaginary part with respect to the real part of the complex signal, the experimental FRF appears circular at the vicinity of a resonance mode. A circle-fit method was used for each mode to measure its resonance frequency ω_r and its modal loss factor η from the circle parameters described in Fig. 2 b. Thus:

$$\eta = \frac{\omega_a^2 - \omega_b^2}{\omega_r\left(\omega_a \tan\left(\frac{\theta_a}{2}\right) + \omega_b \tan\left(\frac{\theta_b}{2}\right)\right)} \quad (1)$$

where $\omega_a,\omega_b,\omega_r,\theta_a$ and θ_b are illustrated in Fig. 2 b [30]. Moreover, for every flexural mode, the Young modulus $\boldsymbol{E}$ of the laminate was calculated by Ref. [31]:

$$E = \frac{12\rho l^4 f_n^2}{e^2 C_n^2} \quad (2)$$

with $\boldsymbol{\rho}$ the density of the composite, l the length of the beam, $\boldsymbol{f_n}$ the average resonance frequency of the n^{th} flexural mode, e the thickness of the beam and $\boldsymbol{C_n}$ a constant depending on the boundary conditions for the n^{th} flexural mode, with $C_1 = 0.55959$, $C_2 = 3.5069$, $C_3 = 9.8194$ and $C_n = (\pi/2)(n-0.5)^2$ for $n>3$ [29].

3. Vibration behaviour of the sandwich components

3.1. Composite skins

First, the influence of the fibre orientation on the vibration behaviour of the composite was studied. Specimens UD-90, UD-45

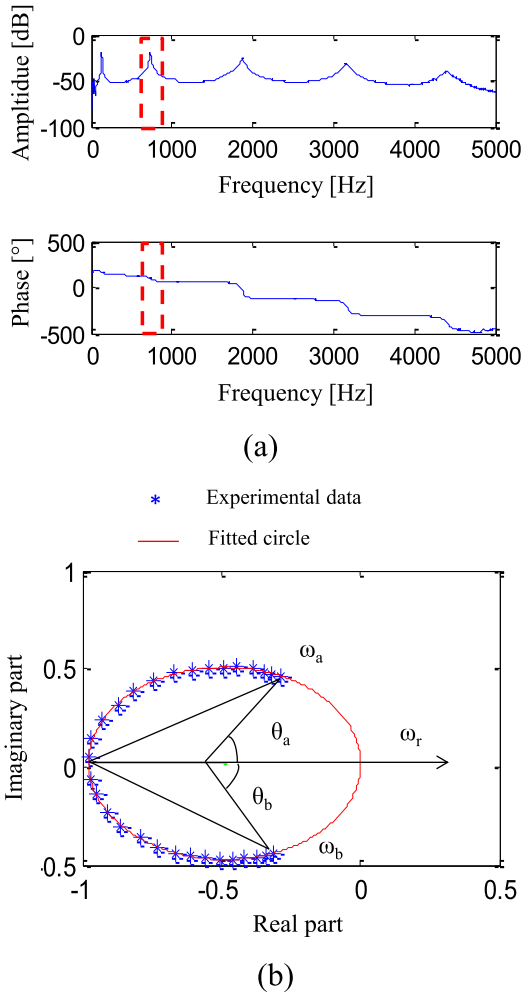

Fig. 2. a) Bode diagram of a typical FRF obtained for a sandwich structure and b) Nyquist diagram of the second mode.

and UD-0 were compared to pure resin specimens. The evolution of their loss factors with frequency is presented in Fig. 3. Composites UD-90 and UD-45 exhibit a similar behaviour. The loss factor is initially very high (6%), close to one of pure resin, and drastically decreases in the frequency range [0 Hz-500 Hz]. Beyond this point the loss factor still decreases but slowly to a quasi-asymptotic value of nearly 4%. Indeed, due to the fibre orientations with respect to the flexural direction, the viscoelastic behaviour of the matrix is predominant. On the other hand, the UD-0 configuration exhibits a very short initial decrease of the loss factor, followed by a quasi-constant phase (around 1.8%) from 500 to 5000 Hz. In this configuration, the reinforcement is 100% in the flexural direction. As a consequence, the beam is much stiffer. This is clearly visible in Fig. 3 b, which presents the evolution of the Young modulus with the frequency. For every specimen, the stiffness measured at low frequency corresponds to the quasi-static Young Modulus presented in Table 1. For UD-90, it is close to 3 GPa, which corresponds to the quasi-static or low frequency Young modulus of pure resin. The modulus of UD-45 appears to be slightly higher.

Then, two cross-ply laminates were studied and compared to the UD-0 beams to see the influence of the stacking sequence. The evolutions of the loss factors and Young modulus with frequency are presented in Fig. 4. As for UD-90 and UD-0 configurations, $[+45/-45]_s$ specimens exhibit a frequency dependent behaviour

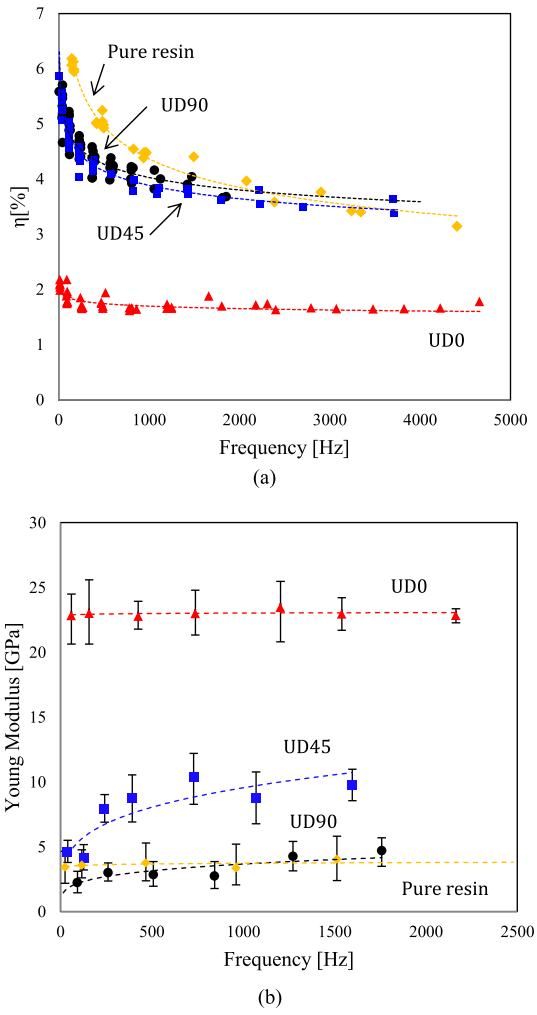

Fig. 3. Evolution of dynamic properties with frequency of UD and pure resin specimens: a) loss factor and b) Young modulus.

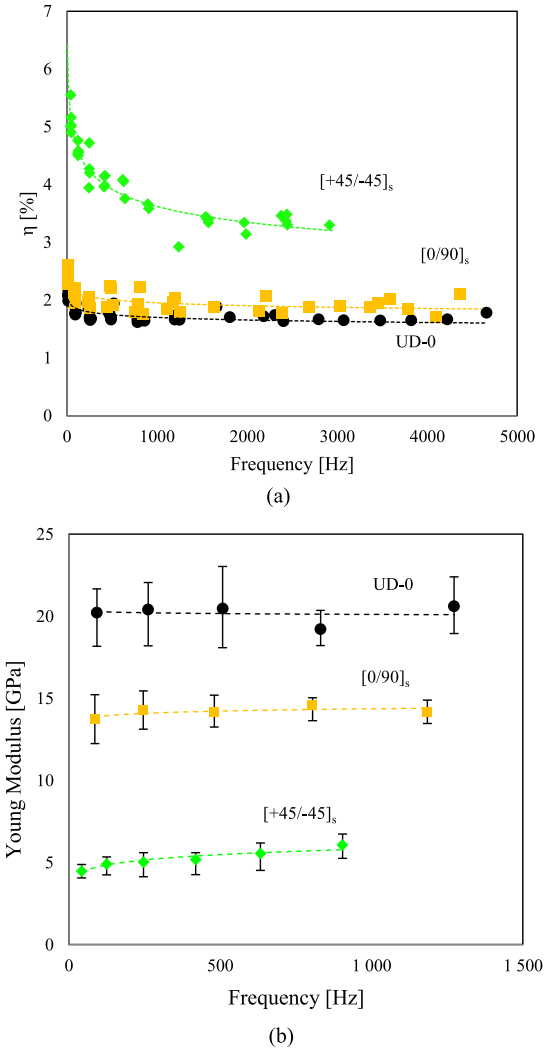

Fig. 4. Evolution of dynamic properties with frequency of cross-play laminates with different stacking sequences: a) loss factor and b) Young modulus.

with an initial decrease of the loss factor (from 5.5% to 3.5% at 3000 Hz) and a slight stiffness increase. Once again, the viscoelastic behaviour of the matrix is predominant due to the fibre orientation. On the other hand, the $[0/90]_s$ specimens behave like UD-0 beams. Its loss factor is slightly higher because of a smaller fibre fraction in the flexural direction Fig. 4 b shows that its static Young modulus is nearly constant equal to13 GPa.

3.2. *Balsa core*

To investigate the dynamic behaviour of the balsa core, two experimental tests were carried out. First, the longitudinal properties of rigid wood beams (without regular cuttings) with nominal dimensions 300 mm × 40 mm × 15.9 mm were measured with the test method described previously. The balsa beams were fixed to 40 mm long metallic fixtures to avoid damaging them by clamping. The results are presented in Fig. 5 a. The loss factor remains nearly constant, equal to 2%. The Young modulus of the balsa beams appears to be constant as well, close to its quasi-static value of 80−100 MPa. The scattering of the results can be explained by the local variations of volume mass in the balsa beams. In fact, balsa wood panels are an assembly of several rectangular wood pieces coming from different trees. As a consequence, they exhibit different densities and different mechanical properties.

Then, a second experimental test was carried out to measure the shear dynamic properties of the beams. Shear is the major sollicitation of a sandwich core subjected to flexure. To achieve this, the Vibration Beam Technique (VBT) was applied [29]. This technique is often used to measure the damping properties of viscoelastic materials. It consists in measuring the resonance frequencies and modal loss factors of a sandwich beam with rigid faces (usually metallic skins), and with a core made of the damping material to be studied. The same properties are measured for the faces separately. Then, the shear modulus G_c and the loss factor η_c of the damping material can be deduced by:

$$\eta_{\downarrow}c = (A\eta_{\downarrow}s) \Big/ \Big(\big((A-B-2)(A-B)^{\uparrow}2 - 2(A\eta_{\downarrow}s)^{\uparrow}2 \big) \Big) \tag{3}$$

$$G_c = P_1 P_2 \tag{4}$$

with:

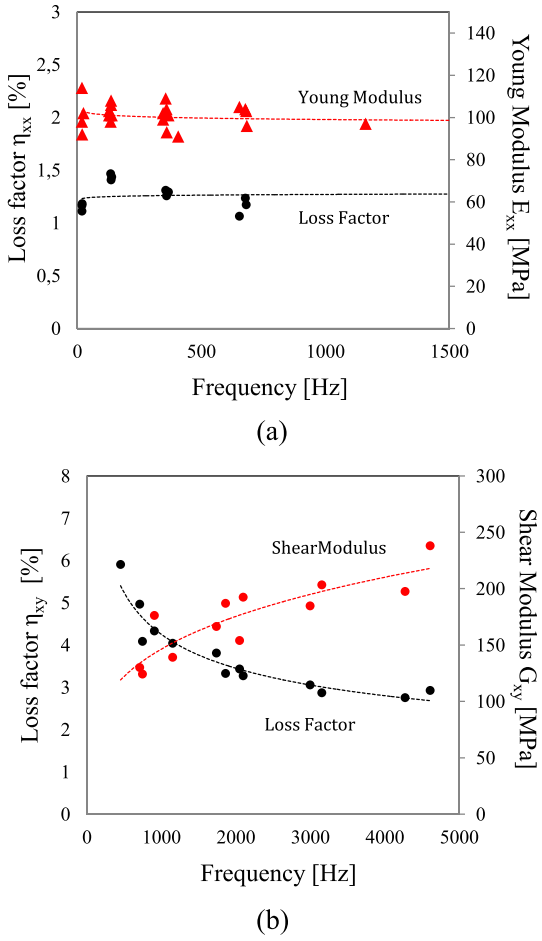

Fig. 5. Dynamic properties of balsa wood: a) longitudinal direction and b) shear direction.

$$P_1 = \left(A - B - 2(A-B)^2 - 2(A\eta_s)^2\right)$$
$$P_2 = \left(\frac{\frac{2\pi C_n E h_f h_c}{l^2}}{\left((1-2A+2B)^2 + 4(A\eta_s)^2\right)}\right) \quad (5)$$
$$A = \left(\frac{f_s}{f_n}\right)^2 \left(2 + \frac{Dh_c}{h_f}\right)\left(\frac{B}{2}\right) \& B = \frac{1}{6\ \ 1 + \frac{h_c}{h_f}}^2$$

where: $D = \frac{\rho_c}{\rho_f}$, E is the Young modulus of the faces, f_n its resonance frequency for mode n, f_s the resonance frequency of the sandwich beam, h_c the thickness of the core, h_f the thickness of a skin, l the length of the beam, η_s the loss factor of the sandwich beam, ρ_c and ρ_f the densities of the core and skins.

Fig. 5 b presents the evolution of the balsa core shear modulus and loss factor with frequency. It is worth noting that the shear properties of the core are very frequency dependent. The shear modulus is initially close to its quasi static value equal to 160 MPa (according the supplier datasheet) and increases to 250 MPa at 5000 Hz. On the other hand, the loss factor is initially close to 6% and decreases to 3% at 5000 Hz. However, low frequency values corresponding to the first flexural mode were not considered as recommended by the VBT test method [29]. In fact, the equations for calculating the damping properties of the core from sandwich beam tests were developed and solved using sinusoidal expansion for the mode shapes of vibration. This approximation is acceptable only for the higher modes. Thus, the first flexural mode is commonly ignored.

3.3. Vibration behaviour of the sandwich structures

Then, the vibration behaviour of sandwich beams made of a balsa wood core and flax/Elium® composite as skins were studied. Four sandwich beam configurations were tested with four core thicknesses (6.4 mm, 12.7 mm, 15.9 mm and 19.1 m). The dynamic loss factors of these beams were measured with the experimental setup described in 2.2. The results are presented in Fig. 6. For all the beams, an initial decrease of the loss factor is noticed. Moreover, it appears clearly that whatever the frequency, an increase of the core thickness results in an increase of the global damping. This can be explained by the important shear loss factor contribution of the core to the damping properties of the whole sandwich structure. It is worth noticing that the statistical spread of the data increases with frequency. This remark will be explained later.

3.4. Discussion

Several hypotheses can be proposed to explain the frequency dependent behaviour and the damping properties of composite and sandwich beams. First, the Elium® thermoplastic resin is a polymer whose viscoelastic behaviour contributes widely to the global response of laminates. It represents 65% of the total volume fraction. Thus, part of the vibration energy is dissipated through friction mechanisms between long polymer chains. Moreover, the reinforcement also contains several viscoelastic components. Flax fibres are composed of natural polymers, such as cellulose (70%), hemicellulose (15%), lignin (2.5%) and pectines (1%) [3],with viscoelastic behaviours. At the composite scale, defects such as micro porosities and weak fibre/matrix interfaces, detected for this composite in previous studies [28] may also contribute to energy dissipation through matrix/matrix and matrix/fibre friction. Moreover, fibre/fibre friction may also occur inside technical fibres. As a matter of fact, elementary fibres are sometimes not impregnated by the matrix where their densities are the highest: inside the bundles. At the sandwich scale, all the previously listed dissipation mechanisms can contribute to the global damping of the

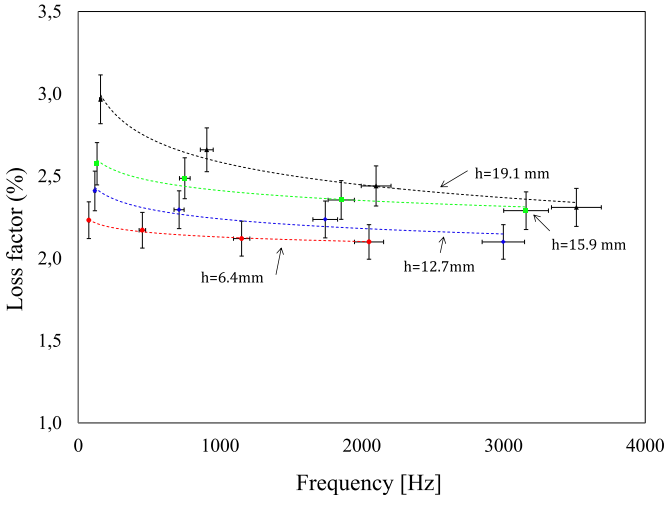

Fig. 6. Influence of core thickness on the loss factor of Flax/Elium/Balsa sandwich beams.

structure, due to the tensile/compressive sollicitation of the skins. The core also participates, due to the viscoelastic behaviour of its natural components. Balsa is also made mainly of cellulose, hemicellulose and lignin. Moreover, due to its cellular microstructure and to the regular cuttings of the panel, a certain amount of resin is trapped in the core during the resin infusion process. This certainly contributes to the global loss factor of the sandwich structures.

4. Finite elements modelling

Several numerical methods can be found in the literature to model or simulate the damping behaviour of sandwich structures. Ross-Kervin-Ungar model [32] is among the first theories developed for this purpose, particularly for constrained layer damping systems. Modal Strain Energy methods, introduced by Adams and Bacon [32–34], has also been widely used [35,36]. Coupled with finite element analyses, it makes it possible to calculate the amount of energy dissipated in the different directions and for the different plies of laminates or sandwich structures. The complex eigenvalue method [37,38] is also commonly used. The resolution of complex eigenvalue problems makes it possible to determine simultaneously both resonance frequencies and modal damping coefficients. Among recent works, some authors have also proposed new procedures to model functionally graded Kirchhoff plates with viscoelastic constitutive behaviours [39–41].

To understand the contribution of the skins and core to the global response of sandwich beams, the MSE method was chosen. A finite element model was created with ABAQUS. To take into account the anisotropic viscoelastic behaviour of the different materials, a MATLAB subroutine was written to modify the material properties with frequency. The method used here consists in: (i) determining the resonance frequencies of every flexural mode, (ii) performing an MSE analysis for every mode considered separately to calculate the elastic and dissipated energies in the skins and in the core in the different directions and (iii) calculating the global loss factor of the whole sandwich beam.

4.1. Presentation of the model and resonance frequencies determination

The sandwich beams were modeled through the thickness with 4-node bilinear plane stress quadrilateral elements, labeled as CPS8 in Abaqus. . The meshed structure with its main geometrical properties is presented in Fig. 7. The total length (of the unclamped part of) the beam is 300 mm. The face thickness h_f were set to 1.6 mm, and the core thickness h_c was changed from 6.4 mm to 19.1 mm to reproduce the different beam configurations studied previously. As a consequence, after a mesh convergence study, 150 elements were defined for each skin. Depending on the core thickness, the number of elements used to mesh the core was set from 600 (for 6.4 mm cores) to 1650 (for 19.1 mm cores). First, the following material properties were defined for the composite faces:

$$\begin{aligned} E_x^f &= 14\ GPa \\ E_y^f &= 3.3\ GPa \\ \nu_{xy}^f &= 0.35 \\ G_{xy}^f &= 1.5\ GPa \end{aligned} \tag{6}$$

They correspond to the quasi-static properties of $[0/90]_s$ composites. The transverse modulus of the unidirectional ply (given in Table 1) was used to define the transverse modulus of the faces. The Poisson's ratios of the matrix and the faces were considered equal. Moreover, the transverse shear modulus was set equal to the shear modulus of the unidirectional ply. For the balsa core, the following material properties were used:

$$\begin{aligned} E_x^c &= 80\ MPa \\ E_y^c &= 3\ GPa \\ \nu_{xy}^c &= 0.1 \\ G_{xy}^c &= 130\ MPa \end{aligned} \tag{7}$$

Quasi-static values of E_x^c and G_{yz} are given in 3.2. Moreover, E_y^c and ν_{xy} were determined according to the literature, [42,43]. The influence of all of these parameters (for faces and core) will be discussed later.

To determine the resonance frequencies of the sandwich structure, the Lanczos solver [44] was used on ABAQUS to solve the real eigenvalues problem of the undamped beam expressed by:

$$\left(K(0) - \omega_0^2[M]\right)\{q\} = 0 \tag{8}$$

where $K(0)$ is the stiffness matrix at 0 Hz defined for the previous material properties, $[M]$ the mass matrix and q the nodal variables. However, this method does not take into account the viscoelastic properties of the materials, leading to underestimated values of the resonance frequencies. Thus, based on the previous experimental results presented in 3.1 and 3.2, power-law fittings of E_x^f and G_{xy}^c frequency evolutions were calculated:

$$\begin{aligned} E_x^s &= 10,4.10^3 f^{0.27} \\ G_{xy}^c &= 24.18\, f^{0.27} \end{aligned} \tag{9}$$

In this sandwich beam configuration, the skins are supposed to support the tensile and compressive axial stresses, and the core is mainly subjected to shear. As a consequence, all other material properties were kept constant with frequency and equal to their quasi-static values mentioned previously. The functions given in Eq. (9) were implemented in a MATALB routine which calculates the materials properties (and the stiffness matrix K) for the resonance frequencies calculated previously at 0 Hz. Then, the real eigenvalue problem was solved with these new material properties. This iterative process was repeated until convergence was achieved for each flexural mode considered separately. Fig. 8 illustrates the convergence of this method for a sandwich beam with h_c = 15.9 mm. It appears that for all modes a limited number of iterations are sufficient to converge at a constant value very close to the

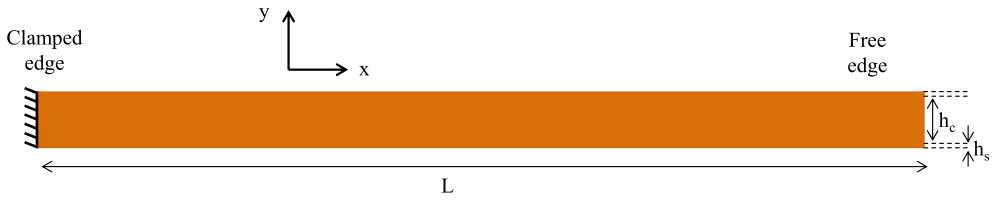

Fig. 7. Geometrical parameters of the meshed finite elements model.

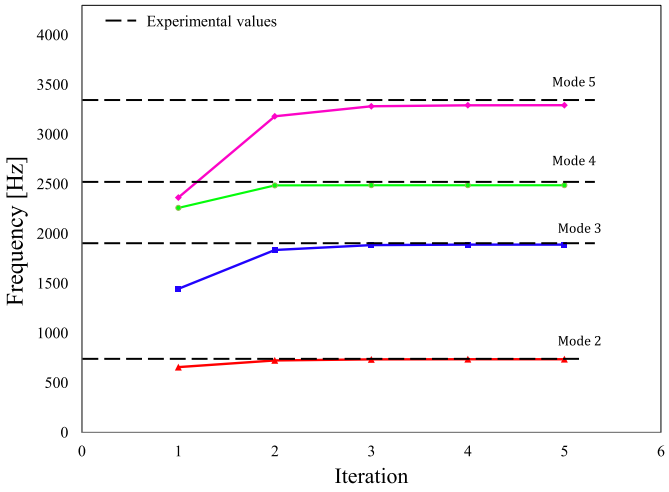

Fig. 8. Convergence of the iterative routine to calculate the resonance frequencies of a sandwich beam.

experimental resonance frequencies. The differences between numerical and experimental results increase with the mode number. They could probably be reduced by the use of more experimental data to affine the power-law fittings proposed in Eq. (9) over a wider frequency range.

4.2. Calculation of elastic energies

Once the resonance frequencies were determined, every mode was considered separately. Stress and strains fields calculated by ABAQUS were analysed by an automatic routine which calculates the elastic energies of the skins and core in the different directions. For a finite element e, the total elastic energy of the element is calculated by:

$$U^e = U^e_{xx} + U^e_{yy} + U^e_{xy} \tag{10}$$

with:

$$\begin{aligned} U^e_{xx} &= \frac{1}{2}\iint_e \sigma_{xx}\varepsilon_{xx}dxdy \\ U^e_{yy} &= \frac{1}{2}\iint_e \sigma_{yy}\varepsilon_{yy}dxdy \\ U^e_{xy} &= \frac{1}{2}\iint_e \sigma_{xy}\varepsilon_{xy}dxdy \end{aligned} \tag{11}$$

Then, the elastic energies of component p (faces f or core c) in the different directions can be calculated by summing the energies of the different elements constituting the component in the different directions by:

$$\begin{aligned} U^p_{xx} &= \sum_{e \in p} U^e_{xx} \\ U^p_{yy} &= \sum_{e \in p} U^e_{yy} \\ U^p_{xx} &= \sum_{e \in p} U^e_{xy} \end{aligned} \tag{12}$$

Finally, U^p the total elastic energy of the component p and U^s the total elastic energy of the sandwich structure are given by:

$$\begin{aligned} U^p &= U^p_{xx} + U^p_{yy} + U^p_{xy} \\ U^s &= U^f + U^c \end{aligned} \tag{13}$$

For the sandwich beam with core thickness $h_c = 15.9$ mm discussed previously, the elastic energies of the skins and core in the different directions are presented in Fig. 9. It appears clearly that U_{xx} represents the major part of the skins' elastic energy, and U_{xy} the major part of the core's elastic energy. As a matter of fact, faces are mainly subjected to tension/compression stresses, whereas the core is subjected to shear. This confirms that the definition of frequency independent material properties out of these directions may not lead to a significant error in the final results. This point has been verified by a preliminary parameters influence analysis.

4.3. Dissipated energies and global loss factor

Finally, the energy dissipated by the skins and core in the different directions was calculated based on the previous experimental results and energy calculations. Considering a finite element e of a component p, the global quantity of dissipated energy is given by:

$$\Delta U^e_p = \psi^p_{xx}U^e_{xx} + \psi^p_{yy}U^e_{yy} + \psi^p_{xy}U^e_{xy} \tag{14}$$

where $\psi^p_{ij} = 2\pi\eta^p_{ij}$ can be deduced from the previous experimental results. Thus, the quantity of energy dissipated in the faces and in the core is:

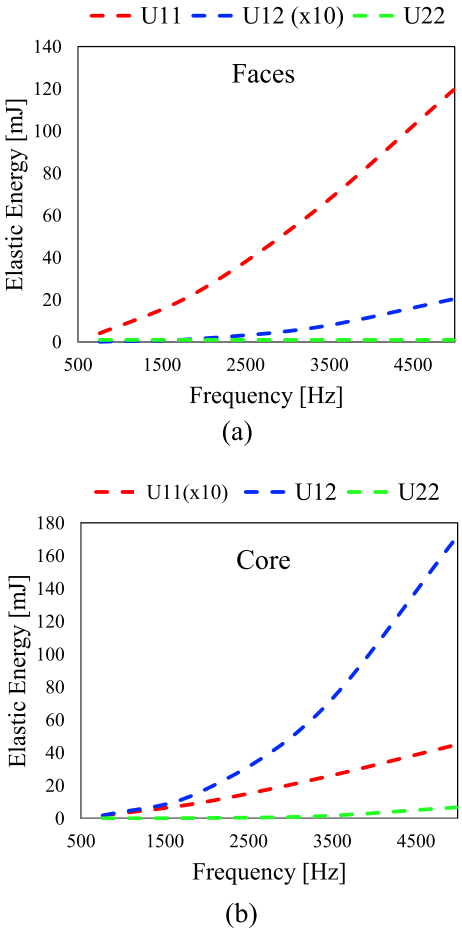

Fig. 9. Elastic energy in the different directions for the different components: a) composite faces and b) balsa core.

$$\Delta U_f = \sum_{e \in f} \Delta U_f^e$$
$$\Delta U_c = \sum_{e \in c} \Delta U_c^e \quad (15)$$

Finally, the quantity of energy dissipated by the whole sandwich beam is given by:

$$\Delta U_s = \Delta U_f + \Delta U_c \quad (16)$$

and the beam global loss factor is.

$$\psi = \frac{\Delta U_s}{U_s} = 2\pi\eta \quad (17)$$

Based on the previous experimental results, power-law fittings of the evolution of η_{xx}^f and η_{xy}^c with frequency were determined. For the faces, the loss factor of the resin was assigned to the transverse and shear directions. Moreover, η_{xx}^c and η_{yy}^c were set equal to the low frequency loss factor of balsa beam measured in 3.2. Thus, the following properties were assigned to the faces and core:

$$\begin{aligned} \eta_{xx}^f &= 2.2f^{-0.016} \\ \eta_{xy}^c &= 0.3403\, f^{-0.301} \\ \eta_{yy}^f &= \eta_{xy}^f = 0.06 \\ \eta_{xx}^c &= \eta_{yy}^c = 0.018 \end{aligned} \quad (18)$$

Preliminary trials confirmed that these parameters, considered constant with frequency, have a negligible influence on the final results, due to the very small fraction of elastic energy associated with these directions.

It was necessary to perform the previous calculations for each flexural mode. Thus, the evolution of the loss factor with frequency was determined for the 4 sandwich beam configurations studied previously. A comparison between numerical and experimental results is presented in Fig. 10. Numerical results appear closely correlated to the experimental measurements. Numerical results are closely correlated to the experimental measurements. The biggest difference appears at low frequency for the thickest sandwich beam. In point of fact, the Modal Strain Energy method is notorious for being not very reliable at lower frequencies, overestimating in some cases the experimental loss factors. The experimental setup, leading to imperfect boundary conditions tends to affect the lower modes. Poor clamping conditions on the root section of the beam can contribute to the total measured damping of the test specimen [29]. As a consequence, results obtained from for the first flexural modes were ignored as explained in 3.2. Several modifications have been proposed to improve the efficiency of this method [45–48]. Moreover, a better correlation could be achieved by using more experimental data to fine-tune the power-law fittings proposed in Eq. (9) and Eq. (18), particularly for low frequencies. The glue (ISOBOND, provided by SICOMIN) used to bond the metallic clamping fixtures to the beams may also influence the results. Other test methods, such as dynamic mechanical analysis (DMA) should be performed to determine more precisely the low frequency shear damping properties of balsa wood.

Then, the fraction of energy dissipated by the skins and the core was calculated for different frequencies and for every sandwich configuration. The results are presented in Fig. 11. For all beams, the skins dissipate the largest fraction of energy for the lowest frequencies. Then the energy dissipated by the skins decreases and that dissipated by the core increases with frequency. This may explain the increase of the statistical spread noticed in 3.3. The balsa core is composed of several wood pieces exhibiting different densities and mechanical properties. Thus, standard deviation of the experimental measurements performed on sandwich beams increases with frequency, because the core becomes more subjected to shear loadings. Moreover, the frequency for which the quantity of energy dissipated by the skins and the core is equal decreases with the thickness of the core. Such a parametric analysis could be used to optimize the dimensioning of the sandwich

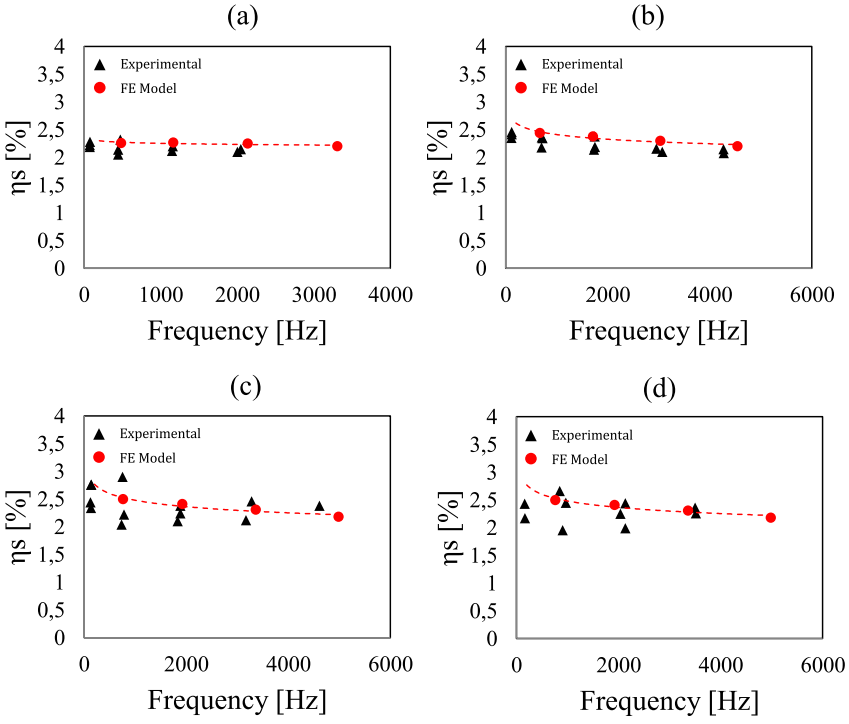

Fig. 10. Evolution of sandwich loss factors with frequency, comparison between experimental and numerical results for different core thicknesses: a) 6.4 mm, b) 12.7 mm, c) 15.9 mm and d) 19.1 mm.

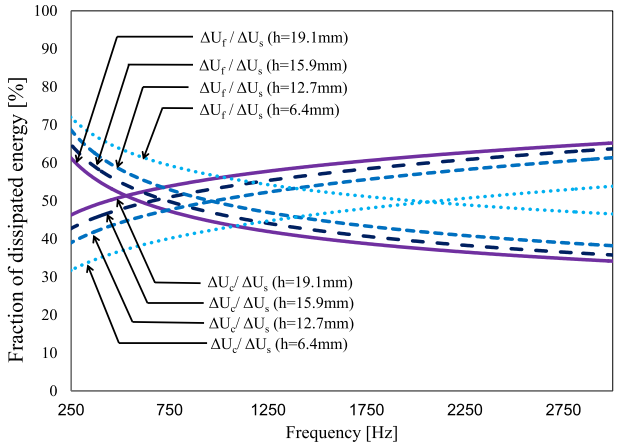

Fig. 11. Fraction of dissipated energy by the core and skins. Parametrical analysis on the influence of the core thickness.

structures to optimize their damping to mass ratios for specific frequencies.

5. Conclusions and perspectives

In this study, the flexural vibration behaviour of bio-based sandwich and laminates beams has been discussed.

Several free vibration tests were performed on different configurations of unidirectional and cross-ply composites to investigate the damping properties of the faces. Then, the dynamic properties of the balsa core were studied as well. Moreover, the damping properties of sandwich structures with different core thicknesses were measured. In addition, a finite elements model was used to determine the resonance frequencies and modal loss factors of the different sandwich beams. The numerical results appeared to be quiet closely correlated to the experimental properties. Thus, the model was used to investigate the contribution of the different components (faces and core) in the global damping response of the sandwich structures. The following conclusions seem to hold:

(i) Elium resin exhibits a frequency dependent loss factor initially close to 6%, which becomes nearly constant equal to 3% for high frequencies. It plays an important role in the damping properties of laminates, particularly for UD composites with unaligned fibres. In addition, the loss factor achieved for the stiffest specimens (UD-0) is close to 2%. Moreover, for all laminates, the damping factor appears to be the highest for low frequencies. After a rapid initial decrease, it tends to become constant for higher frequencies.

(ii) The balsa core exhibits viscoelastic shear behaviour with a high shear loss factor at low frequencies (around 5%). The global loss factor of sandwich beams increases as core thickness increases.

(iii) FE analysis confirms that the faces are mainly subjected to tension/compression stresses and that the core is mainly subjected to shear. Therefore, Young's modulus and the loss factor of the skins were considered frequency dependent, as well as the shear modulus and shear loss factor of the core. All other material properties (elastic moduli, Poisson's ratios and loss factors) were considered constant with frequency. All other loss factors appeared to have negligible effects on the flexural damping behaviour of sandwich beams.

Regarding the previous results, it appears possible to use this kind of FE model to perform numerical parameter analyses to optimize the dimensioning of this eco-composite structure. One possible application could be optimization of the damping to mass ratio of the sandwich for a given flexural mode. This would require additional experimental tests to figure out the influence of face thickness, core density, etc.

Acknowledgments

The authors are grateful for the financial support from the MATIERES project and the “Région Pays de la Loire” in France. The authors would also like to thank Pierre GERARD from ARKEMA for his help with the processing of the Elium resin. Moreover, the authors thank Maëlle TORTEROTO, Alexandre LEBRUN, Florian RODRIGUES DO VALE and Shinji SAGET for their participation in the experimental tests.

References

[1] Summerscales J, Virk A, Hall W. A review of bast fibres and their composites: part 3 – modelling. Compos Part A 2013;44:132–9.
[2] Farooq K. Comportement mécanique des composites sandwichs en statique et en fatigue cyclique. Université du Maine; 2003.
[3] Yan L, Kasal B, Huang L. A review of recent research on the use of cellulosic fibres, their fibre fabric reinforced cementitious, geo polymer and polymer composites in civil engineering. Compos Part B 2016;92:94–132.
[4] Li Y, Mai Y, Ye L. Sisal fibre and its composites: a review of recent developments. Compos Sci Technol 2006;60(2000).
[5] Zhu J, Zhu H, Njuguna J, Abhyankar H. Recent development of flax fibres and their reinforced composites based on different polymeric matrices. Mater (Basel) 2013;6:5171–98.
[6] Pil L, Bensadoun F, Pariset J, Verpoest I. Why are designers fascinated by flax and hemp fibre composites? Compos Part A 2016;83:193–205.
[7] Wambua P, Ivens J, Verpoest I. Natural fibres: can they replace glass in fibre reinforced plastics? Compos Sci Technol 2003;63:1259–64.
[8] Baghaei B, Skrifvars M, Berglin L. Manufacture and characterisation of thermoplastic composites made from PLA/hemp co-wrapped hybrid yarn prepregs. Compos Part A 2013;50:93–101.
[9] Bourmaud A, Ausias G, Lebrun G, Tachon M, Baley C. Observation of the structure of a composite polypropylene/flax and damage mechanisms under stress. Ind Crop Prod 2013;43:225–36.
[10] De Arcaya PA, Arbelaiz A. Mechanical properties of natural fibers/polyamides composites. Polym Compos 2009:254–64.
[11] Bos HL, Müssig J, Van Den Oever MJA. Mechanical properties of short flax fibre reinforced compounds. Compos Part A 2006;37(10):1591–604.
[12] Satyanarayana KG, Arizaga GGC, Wypych F. Biodegradable composites based on lignocellulosic fibers - an overview. Prog Polym Sci 2009;34:982–1021.
[13] Tomas B. Manufacturing and applications structural sandwich components of. Compos Part A 1997;28:97–111.
[14] Ning H, Janowski GM, Vaidya UK, Husman G. Thermoplastic sandwich structure design and manufacturing for the body panel of mass transit vehicle. Compos Struct 2007;80:82–91.
[15] Le Duigou A, Deux J, Davies P, Baley C. PLLA flax mat balsa bio sandwich. Manufacture and mechanical properties. Appl Compos Mat. 2011;18:421–38.
[16] Le Duigou A, Deux J, Davies P, Baley C. PLLA flax mat balsa bio sandwich environmental impact and simplified life cycle analysis. Appl Compos Mat. 2012;19:363–78.
[17] Bekisli B, Grenestedt JL. Experimental evaluation of a balsa sandwich core with improved shear properties. Compos Sci Technol 2004;64:667–74.
[18] Grenestedt JL, Bekisli B. Analyses and preliminary tests of a balsa sandwich core with improved shear properties. Int J Mech Sci 2003;45:1327–46.
[19] Atas C, Sevim C. On the impact response of sandwich composites with cores of balsa wood and PVC foam. Compos Struct 2010;93(1):40–8.
[20] Kandare E, Luangtriratana P, Kandola BK. Fire reaction properties of flax epoxy laminates and their balsa core sandwich composites with or without fire protection. Compos Part B 2014;56:602–10.
[21] Prabhakaran S, Krishnaraj V, Senthil M, Zitoune R. Sound and vibration damping properties of flax fiber reinforced composites. Procedia Eng 2014;97:573–81.
[22] Le Guen M, Newman RH, Fernyhough A, Staiger MP. Tailoring the vibration damping behaviour of flax fibre-reinforced epoxy composite laminates via polyol additions. Compos Part A 2014;67:37–43.
[23] Duc F, Bourban PE, Plummer CJG, Mnson JE. Damping of thermoset and thermoplastic flax fibre composites. Compos Part A 2014;64:115–23.
[24] Assarar M, Zouari W, Sabhi H, Ayad R, Berthelot J. Evaluation of the damping of hybrid carbon flax reinforced composites. Compos Struct 2015;132:148–54.
[25] Sargianis JJ, Kim H-I, Andres E, Suhr J. Sound and vibration damping

characteristics in natural material based sandwich composites. Compos Struct 2013;96:538–44.
[26] Khalfallah M, Abbès B, Abbès F, Guo YQ, Marcel V, Duval A, et al. Innovative flax tapes reinforced acrodur biocomposites: a new alternative for automotive applications. Mat. Des 2014;64:116–26.
[27] Baley C, Le Duigou A, Bourmaud A, Davies P. Influence of drying on the mechanical behaviour of flax fibres and their unidirectional composites. Compos Part A Appl Sci Manuf 2012;43(8):1226–33.
[28] Monti A, El Mahi A, Jendli Z, Guillaumat L. Mechanical behaviour and damage mechanisms analysis of a flax-fibre reinforced composite by acoustic emission. Compos Part A 2016;90:100–10.
[29] "ASTM E756–98;: Standard Test Method for Measuring Vibration Damping Properties of Materials."
[30] De Silva CW. Vibration: fundamentals and practice. CRC press; 2006.
[31] Berthelot JM. Composite materials. Springer; 1997.
[32] Ross D, Ungar EE, Kerwin EM. Damping of plate flexural vibration by means of viscoelastic laminates. ASME Struct Damping 1959:49–88.
[33] Adams RD, Fox MAO, Flood RJL, Friend RJ, Hewitt RL. The dynamic properties of unidirectional in torsion and flexure carbon and glass fiber reinforced plastics. J Compos 1969;3:594–603.
[34] Adams RD, Bacon DGC. Measurement of the flexural damping capacity and dynamic young ' s modulus of metals and reinforced plastics. J Phys D Appl Phys 1973;6:27–41.
[35] M. Assarar, A. El Mahi, and J.-M. Berthelot, Damping Analysis of Sandwich Composite Materials, J. Compos. Mater., vol. 43, no. 13, pp. 1461–1486, 209AD.
[36] Berthelot J, Assarar M, Sefrani Y, El A. Damping analysis of composite materials and structures. Compos Struct 2008;85:189–204.
[37] Rikards R, Chate A, Barkanov E. Finite element analysis of damping the vibrations of laminated composites. Comput Struct 1993;47(6):1005–15.
[38] Barkanov E, Chate A. Damping analysis of sandwich strctures. Trans Eng Sci 1994;4:415–22.
[39] R. Baretta and R. Luciano, Exact solutions of isotropic viscoelastic functionally graded Kirchoff plates, Compos. Struct., vol. 118, pp. 448–454, 14AD.
[40] Apuzzo A, Barretta R, Luciano R. Some analytical solutions of functionally graded Kirchoff plates. Compos Part B 2015;68:266–9.
[41] Baretta R, Luciano R. Anaogies between Kirchoff plates and functionally graded Saint-Venant beams under torsion. Contin Mech Thermodyn 2015;27:499–505.
[42] Soden PD, Mcleish D. Variables affecting the strength of balsa wood. J Strain Anal 2015;11(4):225–34.
[43] Forest Products Laboratory. Wood handbook: wood as an engineering material. Agriculture 2010;72.
[44] Lanczos C. An iteration method for the solution of the eigenvalue problem of linear differential and integral operators. J Res Natl Bur Stand 1950;45:255–82.
[45] Assarar M, El Mahi A, Berthelot JM. Evaluation of the dynamic properties of PVC foams under flexural vibrations. Compos Struct 2012;94(6):1919–31.
[46] Gorreparti KM, Rao MD. Analysis of adhesively bonded double-strip joints by the modal strain energy method. J Vibr *Acoust* 1996;118:28–35.
[47] Landi FP, Scarpa F, Rongong JA, Tomlinson G. Improving the modal strain energy method for damped structures using a dyadic matrix perturbation. J Mech Eng Sci Proc Instn Mech Engrs 2002;2016(Part C):1207–16.
[48] Torvik PJ, Runyon B. Modifications to the method of modal strain energy for improved estimates of loss factors for damped structures. Shock Vib 2007;14:339–53.